ACS Sustainable Chemistry & Engineering

Research Article

pubs.acs.org/journal/ascecg

Quinone Reduction in Ionic Liquids for Electrochemical CO_2 Separation

Burcu Gurkan, Fritz Simeon, and T. Alan Hatton*

Department of Chemical Engineering, Massachusetts Institute of Technology, 77 Massachusetts Avenue, Cambridge, Massachusetts 02139, United States

Supporting Information

ABSTRACT: We report the redox activity of quinone materials, in the presence of ionic liquids, with the ability to bind reversibly to CO_2. The reduction potential at which 1,4-naphthoquinone transforms to the quinone dianion depends on the strength of the hydrogen-bonding characteristics of the ionic liquid solvent; under CO_2, this transformation occurs at much lower potentials than in a CO_2-inert environment. In the absence of CO_2, two consecutive reduction steps are required to form first the radical anion and then the dianion, but with the quinones considered here, a single two-electron wave reduction with simultaneous binding of CO_2 occurs. In particular, the 1,4-napthoquinone and 1-ethyl-3-methylimidazolium tricyanomethanide, [emim][tcm], system reported here shows a higher quinone solubility (0.6 and 1.9 mol·L^{-1} at 22 and 60 °C, respectively) compared to other ionic liquids and most common solvents. The high polarity determined through the Kamlet−Taft parameters for [emim][tcm] explains the measured solubility of quinone. The achieved high quinone solubility enables effective CO_2 separation from the dilute gas mixture that is contact with the cathode by overcoming back-diffusive transport of CO_2 from the anodic side.

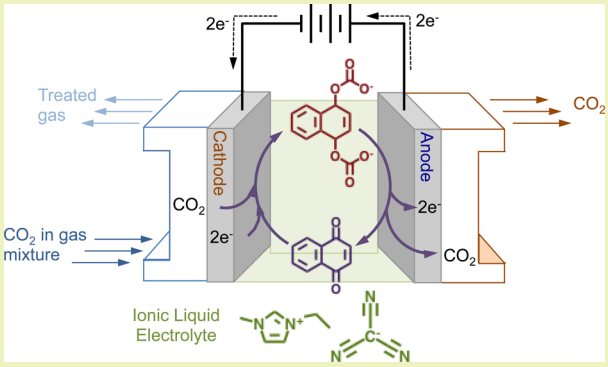

KEYWORDS: *CO_2 capture, Electrochemical separation, Electrochemistry, Quinone, Ionic liquid, Tricyanomethanide, Solvachromatism, Polarity*

INTRODUCTION

The development of new materials and technologies for the reduction of CO_2 emissions from industrial sources remains a significant task if the adverse effects of these emissions on global climate patterns are to be mitigated. To this end, three strategies are being explored: (i) use of renewable energy sources and fuels that are less carbon-rich than the currently favored fossil fuels,[1] (ii) capture and storage of CO_2,[2,3] and (iii) conversion of CO_2 to other useful commodities[4,5] such as cyclic-carbonates,[6] low-density polyethylene,[7] methanol, and formic acid.[1] In this context, electrochemical methods present a viable means for separating and transforming CO_2 because they can be operated under relatively mild conditions (20−60 °C) and can be implemented readily as a direct add-on, drop-in technology. Recent studies on the electrochemical transformation of CO_2 to other chemicals and fuels utilized ionic liquids as the reaction media to avoid the use of harsh solvents, catalysts, and supporting electrolytes.[4,6−10] Such ionic liquids (ILs) have been found to be convenient electrolytes in the electrodeposition of metals, and in batteries and other electrochemical devices, they exhibit negligible volatility, strong electrochemical stability, nonflammability, and a wide liquidus range,[11−13] all of which are desirable properties for CO_2 handling in separations and conversion operations.

In this work, we explore the electrocarboxylation of quinones in ionic liquids for potential applications in the separation of CO_2 from gas mixtures. Quinones are redox-active molecules that have a significantly higher binding affinity for CO_2 in their reduced form than in their neutral state.[14−16] Although the redox behavior of quinones has been studied for many decades because of their importance in chemistry and biological systems,[17−22] very few studies on their electrochemical properties in ionic liquids have been reported. Specifically, in the presence of CO_2, no detailed studies are present. A particularly interesting class of ILs, first reported by MacFarlane et al.,[23] are those containing tricyanomethanide; although they have smaller electrochemical windows compared to most ILs, they have impressively low viscosities (e.g., ∼20 cP at room temperature), which facilitate increased mobility for electroactive species. Data on these ILs are scarce, however, and their potential as electrolytes has not been fully explored.

Carboxylation of quinones in ILs could have significant implications for CO_2 capture applications. Traditional temperature-swing processes for CO_2 capture that utilize aqueous amine absorbents are energy intensive, and it has been

Received: February 17, 2015
Revised: May 13, 2015
Published: May 14, 2015

DOI: 10.1021/acssuschemeng.5b00116
ACS Sustainable Chem. Eng. 2015, 3, 1394−1405

suggested that electrochemical separation methods (ESMs) can provide efficient CO_2 separation from dilute gas mixtures, e.g., postcombustion flue gas or atmospheric gas.[14] The application of ESM can be extended to the reduction of CO_2 levels in confined quarters such as in submarines and spacecraft. ESM operates under benign operating conditions without either the need for intrusive integration within existing power plants or the requirement for a hot steam supply. The basic principles of one possible ESM operation are illustrated in Figure 1.

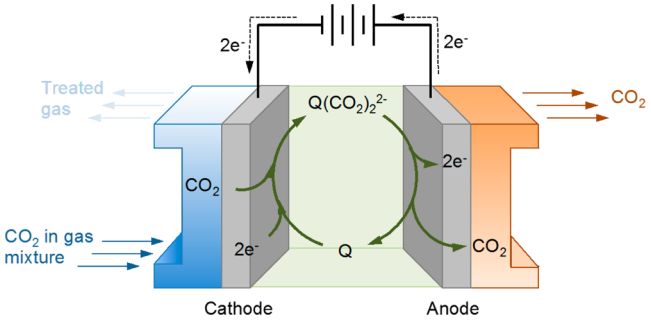

Figure 1. Schematics of an electrochemical CO_2-separation cell utilizing a quinone (Q) redox-active carrier and ionic liquid electrolyte. Electrodes are permeable porous membranes.

In a typical electrochemical cell under consideration for gas treatment, the quinone molecule is reduced at the cathode and binds with CO_2 according to the overall reaction shown in Figure 1. This quinone–CO_2 complex is then transported by diffusion or convection from the cathode to the anode where upon oxidation the quinone complex releases the CO_2. This facilitated transport of CO_2 occurs between the CO_2-lean and CO_2-rich streams at the cathodic and anodic interfaces, respectively. The strength of the quinone–CO_2 affinity depends on the structure of the quinone; some quinones, such as chlorinated anthraquinone and benzoquinone with electron-withdrawing substituents, have weaker complexation with CO_2 than do their unfunctionalized forms or those with electron-donating substituents, such as ether and methyl derivatives.[24] The switchable CO_2 binding is controlled by modulation of the electrode potential. The total CO_2 carrying capacity of quinones is limited by the saturation solubility of the quinone in the solvent, the applied electrode potentials, and the electrode surface areas. Kinetic parameters such as the diffusion coefficients of the complexed and uncomplexed quinone species are dictated by the quinone size and the electrolyte, whereas design considerations ultimately affect the dynamic carrying capacity or diffusional flux. Much attention has been paid to the use of organic solvents, but even under the best of conditions, quinones with short-chain substituents[1] have insufficient solubilities in these solvents (e.g., solubility = 0.33 M for *p*-benzoquinone in dichloromethane,[9] 0.48 M for 1,4-naphthoquinone (1,4-NQ) in toluene[2]). Moreover, evaporative solvent losses and consequent drying of the electrodes reduces the utility of such operations in large-scale applications. Many of these issues could be alleviated if suitable ionic liquids, which characteristically have negligible vapor pressures (no evaporative losses), could be identified that have sufficiently high quinone solubility and reasonable transport properties.

In this study, we report on the properties of ILs as solvents for quinones and, in particular, on their effect on the electrochemical reduction of quinones in the presence and absence of CO_2. The complexation of the reduced quinones with CO_2 facilitates the separation of this dilute greenhouse gas from gas mixtures, whereas the use of ILs avoids the solvent evaporation issues at the electrode surfaces associated with conventional organic solvents. The solvation of quinones depends on the structure and polarity of the ILs in which they are dissolved. We have examined the solubility of selected quinones in different ILs and investigated their redox properties both under inert conditions and when challenged with CO_2. The stability of the quinones under oxygen and in the presence of water, both of which may also be present in the gas mixtures to be treated, was also evaluated. Finally, the transport properties of the quinones in ILs were determined and used to assess the feasible operating regimes of pressure and cell design for the electrochemical separation of CO_2 from feed gas mixtures.

The reduction of quinones in electrolytes based on molecular solvents is well-described by a two-step mechanism in which a radical anion forms in the first step and the dianion on the second reduction step:[20,25]

$$Q + e^- \leftrightarrow Q^{\bullet -} \quad (1)$$

$$Q^{\bullet -} + e^- \leftrightarrow Q^{2-} \quad (2)$$

The potentials at which these reductions occur and the corresponding kinetics of the electron transfer processes depend on the structure of the quinone[17,19,20,26] and its interaction with the electrolyte solvent.[18,22,25,27] In these systems, the supporting electrolyte participates in ion-pairing with the reduced quinones, whereas the polarity of the solvent affects the solvation energies.[17,26,27] In dry, neutral, aprotic media, the two reductions are generally separated by about 0.7 V.[25] Protonation in acidic media and the consequent hydrogen-bonding shift the second reduction to more positive potentials.[18,25] Because of their varying degrees of ionicity,[28,29] ILs, which act as both the electrolyte and the solvent, can have more a specific influence on the quinone reduction than do more conventional solvents.[30] A few studies have reported quinone reduction in imidazolium-based ILs in the solution phase[30−32] and when bound to the electrode surface.[33] In these studies, in order to eliminate the complications associated with metal speciation when using metal-based redox agents, quinones were selected as model redox probes for the evaluation of the IL properties as electrolytes. Quinone reduction in ionic liquids in the presence of CO_2 has not been explored to any great extent in earlier reports.

CO_2 separation from a dilute gas mixture using 2,6-di-*tert*-butyl-1,4-benzoquinone (DTBQ) in 1-butyl-3-methylimidazolium hexafluorophosphate ([bmim][PF_6]) has been demonstrated in a batch-type electrochemical pumping cell.[34] The reported system successfully illustrates the unique concept of concentrating CO_2 by a redox-active quinone carrier, as originally proposed by Dubois et al.[15] No detailed study of the actual redox mechanism in the presence of CO_2 was made, however, and the system performance was limited by the solubility of the quinone in the IL, which was too low for practical applications, and yielded poor separation efficiencies. It was also reported that the reduced quinone used in that study was sensitive to oxygen, the observation of which points to the importance of the potential at which the quinone is reduced and its stability under oxygen to ensure the robustness of a CO_2–ESM process on the basis of these principles. We have, therefore, studied the evaluation criteria for the selection of

DOI: 10.1021/acssuschemeng.5b00116
ACS Sustainable Chem. Eng. 2015, 3, 1394−1405

Table 1. Electrochemical Windows and Viscosities of a Range of ILs[a]

Ionic Liquid	Abbreviation	Structure	η (cP) 295 K	EW (V)	
				under Argon	under CO_2
1-ethyl-3-methylimidazolium bis(trifluoromethylsulfonyl)imide	[emim][Tf_2N]	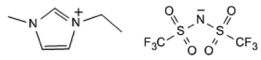	34 [38]	4.1 4.3 [35]	4.2
1-ethyl-2,3-methylimidazolium bis(trifluoromethylsulfonyl)imide	[emmim][Tf_2N]	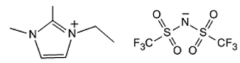	74 [39]	4.6	4.7
1-ethyl-3-methylimidazolium tricyanomethanide	[emim][tcm]	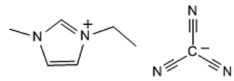	15 18 [40]	3.2 ~3 [23]	3.3
1-ethyl-3-methylimidazolium triflate	[emim][OTf]	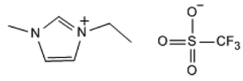	43 [38]	4.2 4.1 [38]	4.3
1-butyl-1-methylpyrrolidinium triflate	[bmpyrr][OTf]	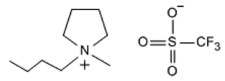	174 [36]	4.2	4.2
1-butyl-1-methylpyrrolidinium bis(trifluoromethylsulfonyl)imide	[bmpyrr][Tf_2N]	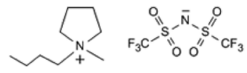	89 [41]	4.2 4.2 [42]	4.3
1-methyl-1-propylpiperedinium bis(trifluoromethylsulfonyl)imide	[mppip][Tf_2N]	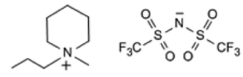	141 [43]	4.5	4.9
butyltrimethylammonium bis(trifluoromethylsulfonyl)imide	[N_{1114}][Tf_2N]	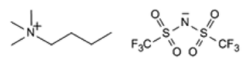	140 [44]	4.7 4.0 [12]	4.7
triethylsulfonium bis(trifluoromethylsulfonyl)imide	[S_{222}][Tf_2N]	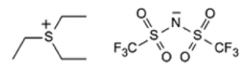	20 [45]	4.3 4.8 [45]	4.2
(ethoxycarbonylmethyl) dimethylsulfonium bis(trifluoromethylsulfonyl)imide	[S_{11ecm}][Tf_2N]	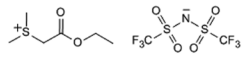	55	3.4	3.4
1-ethyl-2,3-methylimidazolium 2-cyanopyrrolide	[emmim] [2-CNpyr]	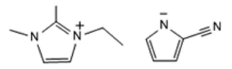	--	2.8	4.8

[a]See refs 12, 23, 35, 36, and 38−45.

redox-active CO_2 carriers such as quinones for electrochemical CO_2 separation and for the IL solvents/electrolytes for these quinones.

EXPERIMENTAL METHODS

Cyclic Voltammetry. Cyclic voltammetry (CV) experiments were performed with a VersaSTAT 3 and 4 potentiostat from Princeton Applied Research. For the electrochemical stability of ILs and the quinone reduction in ILs, a two-electrode system was used in a T-cell as described in the literature.[35] Ag wire was the counter electrode with an 11 μm diameter glassy-carbon working microelectrode. Alternatively, a 10 μm Pt electrode was also used. All of the electrodes were purchased from BASi (Bioanalytical Systems, Inc.). Ferrocene was used as the internal standard, and all of the potentials in the manuscript were standardized by setting the observed half-cell potential for FcIFc+ to 0 V, unless noted otherwise. Approximately 23 μL of sample was used in the T-cell. The environment in the T-cell was controlled by a constant flow of dry argon (99.999%), CO_2 (99,99%), 15% CO_2 balanced with air, or 50% O_2 balanced with Argon as required; all gases were obtained from Airgas.

The hydrogen-bonding affinity between quinones and ILs was studied with a three-electrode system, which consisted of a glassy-carbon working electrode with a 3 mm of diameter, a AglAgCl reference electrode, and a Ag wire as the counter electrode. A 5 mL aliquot of sample was used in this macroelectrode system. The electrolyte consisted of dimethyl sulfoxide (DMSO) with 0.1 M tetrabutylammonium perchlorate (TBAP) as the supporting electrolyte and 1 mM ferrocene as the internal standard. Quinone (5 mM) was dissolved in this electrolyte. The ionic liquid was then introduced to yield concentrations ranging from 1 to 10 mM. Cyclic voltammograms were measured at a 100 $mV{\cdot}s^{-1}$ scan rate before and after each addition of IL.

Solvachromatism. Approximately 3 mL of IL was placed in a cuvette with a stir bar and sealed with a septa cap. Stock solutions of each solvachromatic dye were prepared in dichloromethane (DCM). For each dye, the stock solution was added dropwise to neat IL until a maximum absorbance of ~1 was achieved. Then, the DCM was removed from the sample by evaporation in a heated vacuum oven (60 °C for 2 h). The UV spectra were then again collected with a Thermo Scientific Evolution 220 UV−vis spectrometer.

The $E_T(30)$ parameter is defined as in eq 3 where the maximum absorbance wavelength is that of Reichardt's dye.[36] Kamleft−Taft parameters of ILs were determined as described previously in the literature.[37] Accordingly, the polarizability, π^*, was determined using N,N-diethyl-4-nitroaniline according to eq 4. Hydrogen-bond-accept-

DOI: 10.1021/acssuschemeng.5b00116
ACS Sustainable Chem. Eng. 2015, 3, 1394−1405

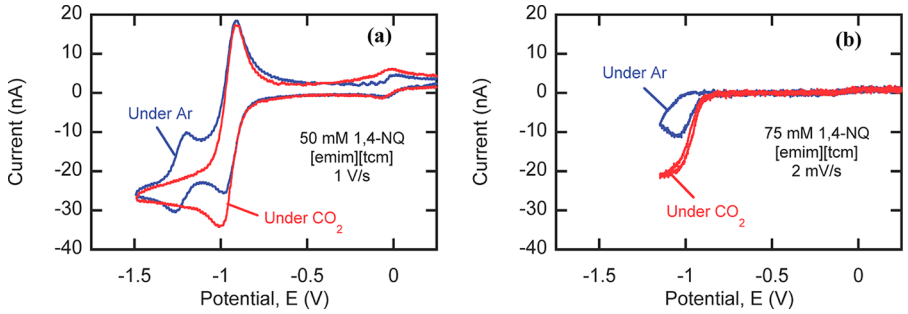

Figure 2. Redox cycle of 1,4-naphthoquinone (1,4-NQ) in [emim][tcm] under argon and CO_2. (a) 50 mM 1,4-NQ at 1 V·s^{-1} and (b) 75 mM 1,4-NQ at 2 mV·s^{-1}. Ferrocene (5 mM) was the internal standard with FcIFc$^+$ set at 0 V. Glassy carbon working electrode, 11 μm diameter, silver wire counter electrode.

ing basicity, β, was determined using 4-nitroaniline and N,N-diethyl-4-nitroaniline according to eq 5. Hydrogen-bond-donating acidity, α, was determined using $E_T(30)$ and π^* values as in eq 6. Phenol blue was used as the polarity indicator when Reichardt's dye was not suitable.

$$E_T(30)\ (\text{kcal·mol}^{-1}) = 28591/(\lambda_{max})_1\ (\text{nm}) \quad (3)$$

$$1/(\lambda_{max})_2 = 27.52 - 3.182\pi^* \quad (4)$$

$$1/(\lambda_{max})_3 = 1.035/(\lambda_{max})_2 - 2.80\beta + 2.64 \quad (5)$$

$$\alpha = 0.0649E_T(30) - 2.03 - 0.72\pi^* \quad (6)$$

Quinone Solubility. A UV−vis spectral calibration curve was constructed using the IL sample with known concentrations of quinone at 22 °C (Figure S6). The samples were diluted in ethanol. Then, a fresh sample of IL was saturated with excess quinone until a precipitate was observed in the mixing vial. A small amount of sample from the liquid phase was then diluted in ethanol to a known concentration. From the UV−vis absorbance obtained for 1,4-NQ in the sample, the solubility limit was calculated.

RESULTS

We have evaluated the physical and electrochemical characteristics of a range of ILs for their suitability as solvents for quinone species that show potential as CO_2 carriers for electrochemical separations. These ILs were screened in terms of their viscosities, quinone solvation capabilities, and electrochemical windows. We further characterized the redox behavior of selected quinones under argon and CO_2 for the most promising of these ILs, relating their reduction potentials to the hydrogen-bonding capabilities of the ILs. The effect of oxygen and water, both of which can be present in gas mixtures from which CO_2 is to be removed, on the redox behavior of the quinones was also investigated.

Electrochemical Stability of ILs. The electrochemical windows of selected ILs with imidazolium, ammonium, pyrrolidinium, piperedinium, and sulfonium cations were measured by CV under argon and CO_2. Table 1 summarizes the measured and literature values for the viscosities at 22 °C and the electrochemical windows of the ILs determined on the basis of a current cutoff criterion of 20 nA.

ILs with bis(trifluoromethylsulfonyl)imide anion are known to be hydrophobic,[46] whereas triflate[47] and cynamides[40,48] are hydrophilic. Sulfonium-based ILs, in general, have low thermal stability and viscosity[41,45,49] compared to imidazolium and phosphonium ILs. Because of the ether linkage in the (ethoxycarbonylmethyl) dimethylsulfonium, [S_{11ecm}], the viscosity of the corresponding IL was expected to be lower than that of an IL with triethylsulfonium, [S_{222}]. Despite its asymmetric structure, [S_{11ecm}][Tf_2N], however, has a significantly higher viscosity than does [S_{222}][Tf_2N] (Table 1). The ionic liquid with the lowest viscosity is 1-ethyl-3-methylimidazolium tricyanomethanide, [emim][tcm], 15 cP at 22 °C. The measured temperature-dependent densities and viscosities for the [S_{11ecm}][Tf_2N] and [emim][tcm] systems are presented in Tables S1 and S2. All the ILs studied are nonreactive toward CO_2, except for imidazolium 2-cyanopyrrolide, whose structure on reaction with CO_2 is altered such that its electrochemical stability increases.

Quinone Reduction Behavior in Ionic Liquids under CO_2. In addition to its low viscosity, [emim][tcm] has the smallest electrochemical window among the ILs studied, with limits of −1.55 and +1.55 V vs FcIFc$^+$ (Figure S1). This narrow window is, however, still able to accommodate the complete redox cycle of 1,4-NQ; this quinone undergoes a two-step reduction to form the 1,4-NQ dianion in [emim][tcm] at half-cell potentials of −0.91 and −1.26 V vs FcIFc$^+$ under argon, as shown in Figure 2a. Under CO_2, only a single wave was observed, at a half-cell potential of −0.96 V. The reaction is reversible as evident from the equality of anodic and cathodic currents in the presence of CO_2 ($i_c \cong i_a$, Figure S2). This was also true for the experiments performed with the microelectrode at slower scan rates, where reaction is no longer diffusion limited. In the absence of diffusion limitations, the forward and reverse scans overlap, and the reduction and oxidation reactions appear as steps rather than separate peaks in the CV.

The complete two-electron reduction of the quinone was easier to accomplish and occurred at a lower electrode potential in the presence of CO_2 than under argon. The single reduction wave observed under CO_2 accounted for the formation of both the semiquinone and the dianion, whereas in the absence of CO_2, two reduction steps were needed to generate the dianion. The current intensity of the observed single wave under CO_2 was much greater than that observed during the formation of the semiquinone under argon. As evident in Figure 2b, where the scan was restricted to not go beyond the first reduction potential at a scan rate of 2 mV·s^{-1}, the current intensity under CO_2 nearly doubled with respect to that under argon at the first reduction potential. This behavior may be due to either the ECE (electrochemical−chemical−electrochemical) mechanism or disproportionation of the semiquinone anion. At the first reduction potential, E_1, the formed semiquinone anion ($Q^{\bullet -}$) reacts with CO_2 (**1**) to form the carboxylated semiquinone anion ($Q^{\bullet}-CO_2^-$). In acidic media and with solvents that form hydrogen bonds, it is reported[25] that the semiquinone anions disproportionate to form the neutral quinone (Q) and its

DOI: 10.1021/acssuschemeng.5b00116
ACS Sustainable Chem. Eng. 2015, 3, 1394−1405

corresponding dianion (Q^{2-}) in the absence of a proton donor. The second electron transfer from the electrode occurs at E_2 to form the dianion. In this study, we observed that the complexation of CO_2 with the quinone caused the second reduction to shift anodically; the degree to which this shift occurred depended on the hydrogen-bonding capability of the solvent. In the case of [emim][tcm], this anodic shift was sufficiently large for both reductions to overlap at E_1. For both mechanisms, an additional molecule of CO_2 was attached (**2**) to yield the saturated carboxylated dianion ($[Q^{-2}CO_2]^{2-}$).

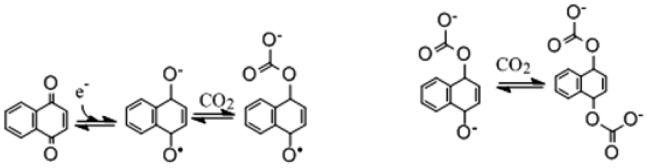

1 **2**

To probe the possible ECE reaction for the 1,4-NQ semiquinone anion in the presence of [emim][tcm] and CO_2, the scan rate was varied between 5 and 100 mV·s^{-1} (Figure S3). The current intensity decreased with decreasing scan rate as steady state was approached, with no changes in the CV profiles. In the case of $[N_{1114}][Tf_2N]$ under CO_2, a second reduction peak emerged when the scan rate was increased from 100 to 1 V·s^{-1}, as seen in Figure 3.

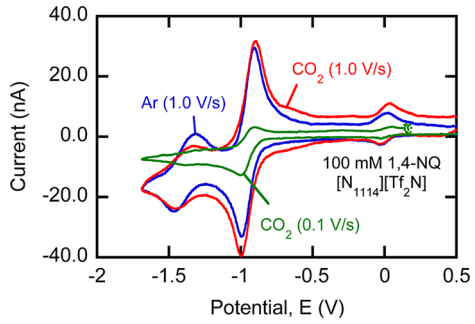

Figure 3. Reduction of 1,4-NQ (100 mM) in $[N_{1114}][Tf_2N]$ under argon and CO_2 at 1 and 0.1 V·s^{-1}. Ferrocene (20 mM) was the internal standard with FcIFc$^+$ set at 0 V.

Because of the high viscosity of $[N_{1114}][Tf_2N]$, the diffusion of the semiquinone anion from the electrode surface was slow so that its concentration at the electrode surface did not change significantly because of mass transfer. At the fast scan rates, the second reduction potential was reached, and the dianion formed before the chemical reaction of $Q^{\bullet-}$ with CO_2 was able to occur. Thus no significant difference was observed in the cyclic voltammograms under argon and CO_2 environments. However, at the slower scan rate of 100 mV·s^{-1}, there was sufficient time at the first reduction potential for reaction of the semiquinone anion with CO_2 to occur, and the enhanced electron delocalization within the quinone facilitated the transfer of the second electron before the second reduction potential was reached. It is important to note that although the first reduction potential of the quinone in $[N_{1114}][Tf_2N]$ was about the same as in the presence of [emim][tcm], the second reduction was at −1.47 V under argon, more negative by 210 mV than in [emim][tcm]. This indicates that $[N_{1114}][Tf_2N]$ has a less of a stabilizing influence on the quinone dianion than does [emim][tcm], which was attributed to its lack of hydrogen-bonding capability.

Effect of H-bonding with Ionic Liquids on Quinone Reduction Potential. The binding affinity between an IL and 1,4-NQ was determined through CV experiments where the IL was introduced in small increments to the DMSO-based electrolyte solution containing the quinone. The corresponding changes in the cyclic voltammograms with the addition of $[emim][Tf_2N]$ are shown in Figure 4a. The first reduction of 1,4-NQ in DMSO at −1.1 V remained unaffected by the addition of the IL, whereas the second reduction potential shifted positively upon this addition. Similar trends were observed with 1,2-naphthoquinone (1,2-NQ, Figure 4b), although the second reduction of 1,2-NQ was electrochemically irreversible, as evident from the decreased intensity of the second oxidation peak. This irreversibility was believed to be due to the much stronger interaction of the $[emim][Tf_2N]$ with the reduced 1,2-NQ than that with 1,4-NQ as a result of the dipole induced by the ortho-positioned oxygens of the 1,2-NQ dianion.

For 1,4-NQ, the strength of association with the IL was calculated from the observed shift in the half-cell potential ($\Delta E_{1/2}$) of the second reduction wave (Figure 5) according to the Nernst equation (eq 7) derived for the IL−1,4-NQ association (Supporting Information), represented as

$$\Delta E_{1/2} = -\frac{RT}{zF}\ln(1 + K_2[\mathrm{IL}]^m) \quad (7)$$

The strength of IL−1,4-NQ association is presented in terms of the number of binding sites, m, and the binding constant, K_2, in Table 2 for the set of ILs studied.

The quinone dianion is a strong hydrogen-bond acceptor, and the hydrogen-bond-donating ability of an IL depends

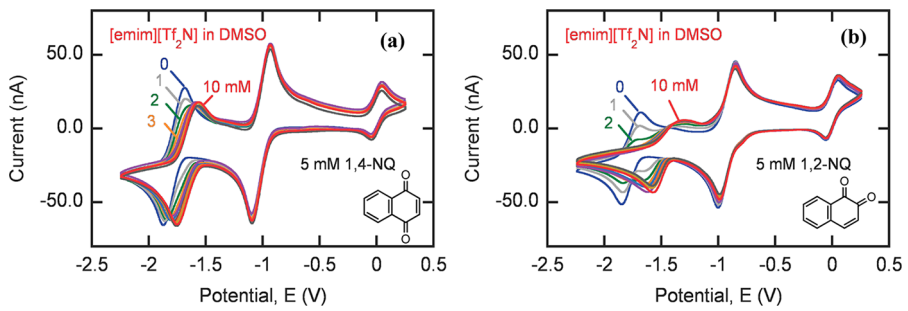

Figure 4. Cyclic voltammetry of 5 mM (a) 1,4-NQ and (b) 1,2-NQ at different concentrations (0−10 mM) of $[emim][Tf_2N]$ in DMSO (0.1 M TBAP, 1 mM Fc). 100 mV·s^{-1} scan rate, AglAgCl reference electrode, 3 mm diameter glassy-carbon working electrode, and silver-wire counter electrode.

DOI: 10.1021/acssuschemeng.5b00116
ACS Sustainable Chem. Eng. 2015, 3, 1394−1405

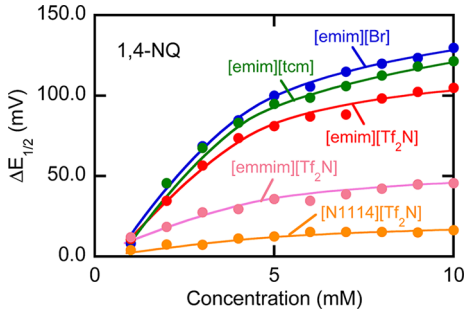

Figure 5. Shift in half-cell of potential of the second reduction of 1,4-NQ in DMSO in the presence of various ILs.

Table 2. Measured Hydrogen-Bonding Parameters for the 1,4-NQ Dianion and the Selected ILs

	m	K_2[IL (mol·L^{-1})]^m
[emim][Br]	2.28 ± 0.11	6.8 (±4.1) × 10^6
[emim][tcm]	2.07 ± 0.10	1.9 (±1.0) × 10^6
[emim][Tf_2N]	1.87 ± 0.11	4.0 (±2.3) × 10^5
[emmim][Tf_2N]	0.91 ± 0.05	3.4 (±0.8) × 10^2
[N_{1114}][Tf_2N]	0.67 ± 0.08	2.1 (±0.8) × 10^1

significantly on its cation. As expected and seen in Table 2, the ammonium-based IL has negligible association with 1,4-NQ relative to that with imidazolium-based ILs. There are two available sites (m = 2) on the imidazolium ILs to interact with 1,4-NQ dianion. When one hydrogen-bonding site on the imidazolium cation is blocked by the methyl group on the α carbon, (i.e., [emmim], with m = 1), the interaction of the IL with the 1,4-NQ dianion is reduced significantly. With increasing anion size, the H-bonding ability of the IL is decreased owing to steric effects, as in the case of [Tf_2N]. It is reported that with increasing anion delocalization, the polarizability of the IL decreases.[50] The [Tf_2N] anion is weakly coordinated with its cation; hence, its solvent strength is weaker than that of [emim][tcm], as also indicated by the lower binding constant, K_2 (where $m \approx 2$).

Solvatochromic Determination of Ionic Liquid Solvent Strength. The solvent strength of [emim][tcm] was determined using solvatochromic probes and is compared with that of [emim][Tf_2N] and other ILs in Table 3. Solvatochromic probes are indicator dyes that exhibit a change in their electron excitation energies according to the polarity of the medium. This change can be observed in the color of the solution or, more sensitively, in its UV−vis spectrum. The general polarity of solvents is often determined using Reichardt's dye 30 and is expressed in terms of the $E_T(30)$ scale, which is a measure of molar transition energy.[36] For ILs, this scale depends mainly on the cation.[51] In acidic media, however, the absorbance band of this dye in the visible range disappears because of protonation/H-bonding;[52] hence, it cannot be used for the determination of the polarity of ILs under these conditions. We therefore used phenol blue as a general IL polarity indicator. The effect of the anion is reflected in the nonspecific interaction parameters for the hydrogen-bond-donating acidity, α, and the hydrogen bond accepting basicity, β. The determination of α, β, and π^*, namely, the Kamlet−Taft parameters, requires the use of different dyes, but α can be calculated using an empirical formula that is based on $E_T(30)$ and π^*. Therefore, for [emim][tcm], an $E_T(30)$ value of 55.2 kcal·mol^{-1} is assumed; this selection was made on the basis of the value for methanol because λ_{max} of phenol blue is similar for both compounds. This is a reasonable assumption because it is in the reported range of $E_T(30)$ values for imidazolium-based ILs. Similarly, for [N_{1114}][Tf_2N], the $E_T(30)$ value for [N_{1888}][Tf_2N] was adopted. The $E_T(30)$ values for tetraalkylammonium-based ILs were found to range from 43 to 51 kcal·mol^{-1}.[52]

The general polarity of [emim][tcm] determined with phenol blue dye is stronger than that of the other imidazolium-based ILs listed in Table 3 with the exception of the IL with the thiocyanate anion. The polarizability parameter, π^*, also indicates a high polarity for [emim][tcm]. Hydrogen-bonding acidity, which is dependent on both $E_T(30)$ and π^*, is the highest for [emim][tcm], whereas that for [N_{1114}][Tf_2N] is more similar to the bonding acidity of [bmmim][Tf_2N]. Because of its strong solvent strength and H-bonding ability, again [emim][tcm] is identified as the preferred IL for further study.

Quinone Solubility and CO_2 Carrying Capacity in [emim][tcm]. The solubilities of neutral 1,4-NQ and 9,10-phenanthraquinone (PQ) in [emim][tcm] were measured using UV−vis spectrometry with a reproducibility of 4%. Table 4 summarizes the solubilities of 1,4-NQ and PQ in [emim][tcm] at temperatures between 22 and 60 °C, from which the

Table 3. $E_T(30)$ (kcal·mol^{-1}), Kamlet−Taft Values, and λ_{max} of Phenol Blue for a Range of ILs

	general polarity, $E_T(30)$	polarizability, π^a	H-bond-donating acidity, α	H-bond-accepting basicity, β	phenol blue λ_{max}
dichloromethane	41.1	0.792	0.066	−0.019	590
dichloromethane[37]	40.7	0.791	0.042	−0.014	588
methanol[37]	55.2	0.600	0.980	0.660	607
[emim][Tf_2N]	53.1[52]	1.021	0.681	0.246	596
[emim][Tf_2N][53]	52.0	0.90	0.76	0.28	
[emim][Tf_2N][54]	52.2	0.97	0.659		
[emmim][Tf_2N][55]	51.8				
[emim][tcm]	55.2[a]	1.166	0.713	0.726	610
[emim][thiocyanate]					614
[bmim][Tf_2N][37]	51.5	0.984	0.617	0.243	
[bmmim][Tf_2N][37]	48.6	1.01	0.381	0.239	
[bmim][OTf][37]	52.3	1.006	0.625	0.464	
[bmim][PF_6][37]	52.4	1.032	0.634	0.207	598
[N_{1114}][Tf_2N]	49.1[b]	0.946	0.477	0.246	586

[a] $E_T(30)$ of methanol is adapted. [b] Polarity of [N_{1888}][Tf_2N][55].

DOI: 10.1021/acssuschemeng.5b00116
ACS Sustainable Chem. Eng. 2015, 3, 1394−1405

Table 4. Measured Quinone Solubilities in [emim][tcm] at Selected Temperatures

	Quinone solubility ($mol \cdot L^{-1}$)			
	22 °C	40 °C	50 °C	60 °C
1,4-naphthoquinone	0.56	0.97	1.34	1.91
9,10-phenanthraquinone	0.17	0.29	0.36	0.54

enthalpies of dissolution were determined to be 37 and 35 $kJ \cdot mol^{-1}$ for 1,4-NQ and PQ, respectively.

The solubility of PQ was observed to be significantly lower than that of 1,4-NQ in [emim][tcm] because of structural steric effects that hindered its solvation by the IL. The reported solubility of DTBQ, which suffers from even more significant steric constraints than does PQ, in [bmim][PF_6] at 27.5 °C is 0.1 $mol \cdot L^{-1}$.[34] We have also observed much lower solubility of this specific quinone in [emim][tcm]. UV−vis analysis for DTBQ/IL was not possible because a quantifiable signature peak could not be identified. Reported values for $E_T(30)$ for [bmim][PF_6] range from 49 to 52.6 $kcal \cdot mol^{-1}$.[52] The general polarity scale for [bmim][PF_6] is similar to that for [emim]-[tcm] and for other imidazolium-based ILs, although the Kamlet−Taft values are lower than those for [emim][tcm]. It is clear that 1,4-NQ in solution is stabilized by [emim][tcm] through H-bonding, which enables this quinone to be dissolved at high concentrations in the IL, an essential need for a practical ESM process. With increasing quinone concentration, the current intensity in the CV experiments increased proportionally as seen in Figure 6a. Similarly, when there was little CO_2 in the gas under which the experiments were performed, the current density decreased. Indeed, with 15% CO_2 in air, the second reduction peak registered because there was insufficient CO_2 dissolved in the IL available to react with all of the reduced quinone. Figure 6b illustrates the CV of 1,4-NQ in [emim]-[tcm] under argon and 15 and 100% CO_2.

Electrochemical Stability of ILs under Oxygen. The reduction of O_2 is a complex process that is dependent on the solvent acidity, the type of electrode, and the presence of other impurities.[56,57] It is possible that superoxide formation takes place at potentials where quinone reduction occurs. Therefore, with a high concentration of quinones present in the IL, the effect of oxygen reduction is unlikely to be observed cleanly in the CV experiments. We did not observe any increase or decrease in the redox currents over 10 repeated cycles within the quinone reduction region after the sample was equilibrated with a 15% CO_2 in air mixture (Figure S4). This repeatability is again evidence that the reaction is both electrically and chemically reversible under these conditions. It is important to recognize that the oxygen solubility is dramatically lower than that of CO_2 in ILs and comparable or lower to that in organic solvents.[58,59] For instance, Brennecke and co-workers[58] reported a Henry's law constant of 3700 bar for O_2 in comparison to 25 bar for CO_2 at 10 °C for [bmim][Tf_2N]. Therefore, it is possible that there was no appreciable amount of O_2 dissolved in [emim][tcm].

To increase the amount of dissolved O_2 in the IL, the sample was saturated with pure oxygen prior to the CV experiments (five cycles, Figure S5). No significant differences were observed between the reduction behavior under O_2 and that under Ar. Because the relatively short O_2 saturation (~2 h) and cycle times may have precluded the presence of sufficient oxygen to cause a detectable effect, we tested an old sample of 1,4-NQ in [emim][tcm] that was kept in a closed vial for several weeks. This old sample appeared much darker than the fresh solutions and showed a significantly reduced current intensity under O_2 (Figure S5). This degradation may have been the result of many factors, including not only the possible instability of the quinone but also absorption of water over a long period of time. Therefore, more investigation is needed in the degradation patterns of quinone in the presence of oxygen, which we leave to a future study.

Effect of Water on Quinone Reduction in [emim]-[tcm]. Not only oxygen but also water can be present in a CO_2-containing gas mixture. Water is a common impurity in ILs and has a negative effect on their electrochemical window: with 10 vol % water, the electrochemical window of [emim][tcm] narrows by 290 mV. Beyond about 10 vol %, the solubility limit of water in the IL may be exceeded, and an inhomogeneous mixture of polar and nonpolar pockets in the sample may result. It is reported that dicyanamide ILs are more hygroscopic than, for example, those with [Tf_2N], but tricyanomethanide ILs are not as hygroscopic.[23] The 1,4-NQ reduction process was observed to be stable in up to 5 vol % water, as seen in Figure 7. The increased current intensity is due to the decrease in viscosity (Table S2) upon the addition of water.

Diffusivity of Quinone in [emim][tcm]. In addition to the quinone solubility and its reduction potential, the diffusivity of the quinone−CO_2 dianion is an important parameter affecting the efficiency of an ESM process that utilizes such redox carriers. The diffusivity (D, in $m^2 \cdot s^{-1}$) of Fc and 1,4-NQ in [emim][tcm] was determined from the steady-state current intensity, i_{ss}, through the equation[7]

$$i_{ss} = 4zFr_dDC \quad (8)$$

where z is the number of electrons, F is Faraday's constant (96 485 $C \cdot mol^{-1}$), r_d (m) is the radius of the electrode, and C is

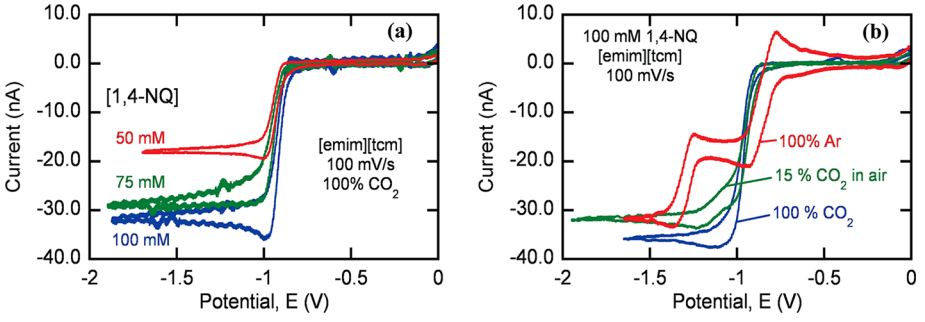

Figure 6. (a) Increasing current intensity with respect to quinone concentration in [emim][tcm] under CO_2. (b) Reduction of 1,4-NQ (100 mM) in [emim][tcm] under argon, 15% CO_2 (balanced with air), and 100% CO_2 at a scan rate of 100 $mV \cdot s^{-1}$.

DOI: 10.1021/acssuschemeng.5b00116
ACS Sustainable Chem. Eng. 2015, 3, 1394−1405

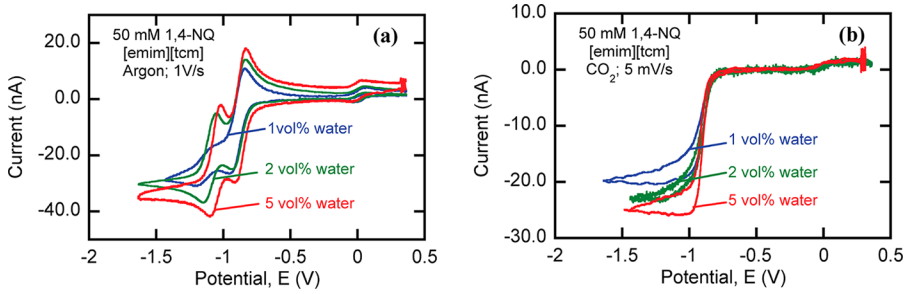

Figure 7. Effect of water on CV of 1,4-NQ (50 mM) with 5 mM Fc in [emim][tcm] under (a) argon and (b) CO_2.

the bulk concentration of the parent species (mol·L^{-1}). To ensure operation in the steady-state operating range the following condition should be fulfilled:[7]

$$p = \sqrt{\frac{Fr_d^2\vartheta}{RTD}} \ll 1 \tag{9}$$

where R is the gas constant (8.314 J·K^{-1}·mol^{-1}), T is the temperature (K), and ϑ is the scan rate (V·s^{-1}). Accordingly, at 293 K with r_d = 5 μm and an assumed $D = 6.9 \times 10^{-11}$ m^2·s^{-1}, the scan rate should be much lower than 50 mV·s^{-1}. In the ionic liquid medium, which is often viscous, true steady-state operation is difficult to attain. The diffusion coefficients given in Table 5 were determined with a scan rate of 2 mV·s^{-1}, with a corresponding p value of 0.18, which suggests that the process was not at true steady state. Therefore, the obtained diffusivities at 2 mV·s^{-1} scan rate should be taken as approximate values.

Table 5. Measured Diffusion Coefficients and Initial Concentrations at 22 °C

	D (m^2·s^{-1})	C (mol·L^{-1})
ferrocene	7.8×10^{-11}	0.01
1,4-naphthoquinone	6.9×10^{-11}	0.1
	6.5×10^{-11}[a]	0.1

[a]Determined by fitting the chronoamperometric response of the first reduction (step ii) to eqs 10−12.

In addition, chronoamperometry was performed with the following sequence: (i) 0 V for 20 s, (ii) −0.60 V for 30 s, (iii) −1.95 V for 30 s, and (iv) 0 V for 10 s with a step time of 0.01 s under argon. Note that these potentials are with respect to an Ag reference using a glassy-carbon microelectrode. With respect to the Fc|Fc$^+$ internal reference, these voltages at steps ii and iii are −0.15 and −1.5 V, respectively, and occur right after the first and second reductions, respectively (Figure 2). The chronoamperometric transient is shown in Figure 8.

The current response at −0.6 V was analyzed using the method of Shoup and Zsabo[60] where the time-dependent current was defined through the following expression:

$$i = -4zFDCr_d f(\tau) \tag{10}$$

$$f(\tau) = 0.7854 + 0.8863\tau^{-0.5} + 0.2146\exp(-0.7823\tau^{-0.5}) \tag{11}$$

$$\tau = 4Dt/r_d^2 \tag{12}$$

The estimated diffusion coefficient, 6.5×10^{-11} m^2·s^{-1} at 22 °C, of the neutral quinone using eqs 10−12 is in good agreement with the previously determined diffusivity using eq 8, as seen in Table 5. From the chronoamperometric transients,

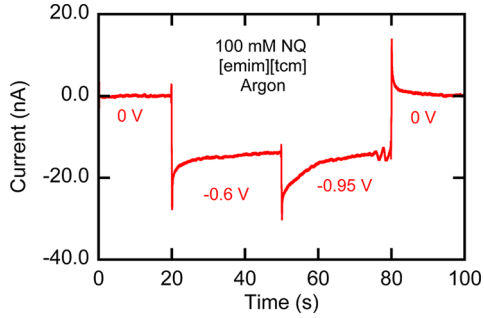

Figure 8. Chronoamperometric response of 100 mM 1,4-NQ in [emim][tcm] under argon, with an 11 μm diameter glassy-carbon electrode. The segments correspond to 0, −0.6, −0.95, and 0 V vs Ag on the glassy-carbon electrode with silver wire as the counter electrode. Time step is 0.01 s.

it is seen that current intensities level off at around 15 nA for both the anion and the dianion. This current yields a diffusion coefficient of about 3.3×10^{-11} m^2·s^{-1} on the basis of eq 8 with the concentration of the neutral quinone assumed to be bulk quinone concentration, although the exact concentration of the reduced species was not known in this case. Although the final currents were similar, the elapsed time to reach steady-state current for the dianion was longer. The initial slow response of the dianion can be attributed to its stronger interaction with the IL. Therefore, it is anticipated that the quinone−CO_2 dianion would also have a diffusion coefficient smaller than that of the neutral quinone. Such differences between the neutral and reduced 1,4-benzoquinone (BQ) were reported previously by Compton et al.[61] Our measurement of the 1,4-NQ diffusion coefficient is in good agreement with that of BQ in [emim][Tf_2N], 4.62×10^{-11} m^2·s^{-1}, when the much lower viscosity of [emim][tcm] is taken into account. (See Table 1.) The reported diffusion coefficients for the reduced forms of BQ in [emim][Tf_2N] are 1.82 and 1.55×10^{-11} m^2·s^{-1} for the semiquinone anion and the dianion, respectively.[61] In [emim]-[Tf_2N], the ferrocene diffusion coefficient has reported values ranging between 3.35×10^{-11}[62] and 6.6×10^{-11} m^2·s^{-1},[63] depending on the exact experimental conditions (e.g., vacuum versus argon atmosphere). An estimation of the diffusion coefficient for 1,4-NQ in the presence of CO_2 was not possible because of the overlap of potentials, as seen in Figure 2.

An Evaluation of 1,4-NQ−[emim][tcm] System for Electrochemical CO_2 Separation. Two major overpotentials are required to operate the ESM process effectively with ionic liquids: one to overcome ohmic losses caused by conduction limitations of the ionic liquid (the ohmic overpotential) and the other to compensate for mass transfer limitations as a result of the high viscosity of the solution (the concentration over-

DOI: 10.1021/acssuschemeng.5b00116
ACS Sustainable Chem. Eng. 2015, 3, 1394−1405

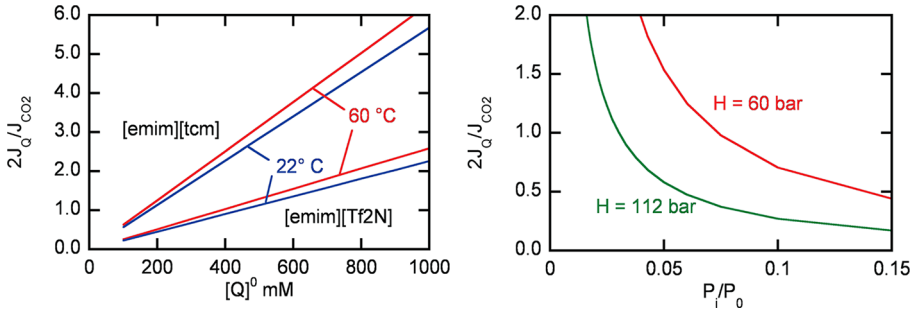

Figure 9. Relation between the (a) achievable ratio of CO_2 flux caused by quinone carrier over the dissolved CO_2 and the quinone concentration and (b) minimum required quinone concentration in the solvent and the ratio of CO_2 partial pressure in the inlet (cathodic) over the outlet (anodic).

potential). The activation overpotential is ignored because there is no deposition on the electrode surface. The ohmic overpotential is dependent on the geometry of the electrodes and the cell setup, whereas the concentration overpotentials can be minimized by agitation and by increasing the bulk concentration of the quinone. It is crucial that the IL be able to solvate sufficient quantities of the quinone to enable efficient reactive capture of CO_2 from the feed gases, but it should not allow for a high physical solubility of CO_2 because this would be detrimental to the separation efficiency. These requirements are due to the transport of CO_2 from the cathode to the anode, which is determined by the concentrations of the reduced quinone–CO_2 adduct at each electrode (high at the cathode, low at the anode) and is counteracted by the diffusion in the opposite direction resulting from the concentration gradient in the physically dissolved CO_2 that is in equilibrium with the gas at each electrode (low partial pressure at the cathode in contact with the feed gas and high partial pressure at the anode in contact with the CO_2-rich gas product stream). Fick's law can be used to describe the flux of the 1,4-NQ–CO_2 adduct ($J_{Q(CO_2)_2^{-2}}$), which is related directly to the flux of the neutral quinone (J_Q) via

$$J_{Q(CO_2)_2^{-2}} = -J_Q \approx D_Q \frac{[Q]^0}{L} \tag{13}$$

and that of molecular CO_2 itself (J_{CO_2}) through

$$J_{CO_2} = -D_{CO_2} \frac{[CO_2]_{anode} - [CO_2]_{cathode}}{L} \tag{14}$$

where $[Q]^0$ is the total bulk concentration of 1,4-NQ, irrespective of oxidation state, and L is the distance between the electrodes. (See Supporting Information for the data and calculations.) It is implicitly assumed here that the reduction and oxidation of the quinone species (and the simultaneous complexation and decomplexation reactions with CO_2) at the cathode and anode, respectively, are instantaneous and that the diffusion coefficients for the oxidized and reduced quinones have the same values. For unidirectional diffusion, the flux of CO_2 from the cathode to the anode caused by the electrochemical process is twice that of the 1,4-NQ–CO_2 dianion ($J_{Q(CO_2)_2^{-2}}$) because 1 mol of quinone carries 2 mol of CO_2. The flux of molecular CO_2 across the cell (J_{CO_2}), caused by the concentration gradient of dissolved CO_2, is given by eq 14, and thus the total flux of CO_2 across the cell is

$$\begin{aligned} J_{CO_2-total} &= 2J_{Q(CO_2)_2^{-2}} + J_{CO_2} \\ &= [2D_Q[Q]^0 - D_{CO_2}([CO_2]_{anode} - [CO_2]_{cathode})]/L \end{aligned} \tag{15}$$

For a net separation of CO_2 from a gas mixture containing 15% CO_2, the minimum required initial quinone concentration, $[Q]^0$, is dictated by the need for the ratio of these fluxes to exceed unity, i.e., for $2(J_{Q(CO_2)_2^{-2}})/J_{CO_2} > 1$. In terms of the partial pressures, P, of CO_2 on either side of the cell, then we require that

$$[Q]^0 > \frac{1}{2}\frac{D_{CO_2}}{HD_Q}\left(\frac{P_{anode} - P_{cathode}}{L}\right) \tag{16}$$

where H is the Henry's law constant, defined by $P = H[CO_2]$. This relation is demonstrated in Figure 9a. At 60 °C, the minimum required concentration of quinone is roughly 200 mM to enable a net flux of CO_2 from the cathode to the anode to be achieved. From another perspective, it can be said that as the CO_2 solubility increases (H decreases) the quinone requirement in the solvent phase increases, as illustrated in Figure 9b. Such a high concentration of quinone with respect to CO_2 is achievable in ILs, specifically [emim][tcm], but not in conventional solvents normally studied for electrochemical separations.

The solubility of CO_2 in [emim][tcm] was estimated by thermal gravimetric analysis (TGA) between the temperatures of 22 and 60 °C. (See Supporting Information for details.) The Henry's law constant at 22 °C is 51 bar with a solution enthalpy of −17 kJ·mol^{-1}. Under atmospheric pressure of CO_2, these values correspond to solubilities of 74 and 5 mM in [emim][tcm] at 22 and 60 °C, respectively. Because the solubility of CO_2 decreases with increasing temperature and vice versa for the quinones, operation at higher temperatures, e.g., at 60 °C, would be more favorable for the CO_2 capture process. However, the stability of the quinones at these temperatures has yet to be established conclusively.

The energetics of the electrochemistry process can be described through the Gibb's free energy as follows:

$$\Delta G = -nF(\Delta E) \tag{17}$$

where n is the number of electron moles transferred, F is Faraday's constant, and ΔE is the potential difference between the oxidation and reduction processes. At the nonstandard state, the Nernst equation becomes

DOI: 10.1021/acssuschemeng.5b00116
ACS Sustainable Chem. Eng. 2015, 3, 1394–1405

$$E = E^0 + \frac{RT}{2F}\left(\ln\left(\frac{[Q^{-2}]_0}{C^0}\right) - \ln\left(\frac{[Q(CO_2)_2^{-2}]}{[Q^{-2}]}\left(\frac{P^0}{P_{CO_2}}\right)^2\right)\right) \quad (18)$$

where $[Q^{-2}]$ and $[Q(CO_2)_2^{-2}]$ are the concentrations of the quinone dianion and the CO_2-complexed quinone dianion, respectively. C^0 and P^0 are the concentration and pressure, respectively, at the standard state. $[Q^{-2}]_0$ is the total concentration of quinone dianion and P_{CO_2} is the partial pressure of CO_2. The term in the second natural logarithm is essentially the equilibrium constant, K_{CO_2}, for the reversible CO_2 absorption by the quinone dianion. Therefore,

$$\Delta E = E_{anode} - E_{cathode} = \frac{RT}{2F}\ln(1 + K_{CO_2}(P_{CO_2})^2) \quad (19)$$

For 1,4-NQ in [emim][tcm] under CO_2, studied here, ΔE = −0.089 V, as observed in Figure 2a. The theoretical energy requirement for the operation of the cell is 17 kJ per mol of CO_2. In practice, there would be inefficiencies because of the overpotentials discussed earlier. We showed that we can achieve quinone concentrations up to 0.56 M at 22 °C. However, not all of the quinones in the reduced state will be able to absorb CO_2 because of the chemical equilibrium. The CO_2 concentration in the liquid that is available to react is dictated by its partial pressure. Furthermore, a fraction of the physically dissolved CO_2 will always be retained in the liquid. If we assume a 40% efficiency, then the electrical energy requirement becomes 43 kJ·mol^{-1}, which is attractive when compared with the requirements of traditional separation processes (145−200 kJ·mol^{-1} of thermal energy which corresponds to 50−70 kJ·mol^{-1} CO_2 electrical equivalent for the absorptive CO_2 capture by amine-based solvents).[64,65]

CONCLUSIONS

We have identified a suitable IL as the electrolyte for the electrochemical separation of CO_2 from a gas stream by a redox-active carrier species with which it can form complexes under appropriate reduction conditions. The IL, [emim][tcm], has been characterized in terms of its interaction with the quinone redox carrier, its electrochemical stability, and its physicochemical properties. 1,4-Naphthoquinone has a higher solubility in the [emim][tcm] system compared to other ILs and most common solvents. The highly polar IL is able to stabilize the reduced form of the quinone through hydrogen bonding. Under CO_2, the quinone reduction in ILs takes place at a single wave that is more positive than that observed with molecular solvents. This suggests that the voltage requirement, and hence the redox window, in electrochemical CO_2 separations utilizing ILs can be significantly reduced without affecting the CO_2 carrying capacity. Although the diffusion coefficients are not as high as would be in the case of organic solvents, the complications arising from the drying of the electrodes because of electrolyte evaporation, instability of both the solvents and the redox carriers, and flammability are addressed by identifying a suitable nonflammable IL that can accommodate a high quinone concentration. Alternative design considerations, such as incorporation of convectional effects within the solvent layer between the two electrodes, can overcome the diffusional limitations of a species migration in the ionic liquids.

ASSOCIATED CONTENT

Supporting Information

Materials, densities, viscosities, cyclic voltammetry, IL−quinone association, CO_2 solubility, and calculation of fluxes. The Supporting Information is available free of charge on the ACS Publications website at DOI: 10.1021/acssuschemeng.5b00116.

AUTHOR INFORMATION

Corresponding Author

*E-mail: tahatton@mit.edu.

Present Addresses

B.G.: Polymer Engineering Department, University of Akron, Akron, Ohio 44325, United States.

F.S.: Research & Development Center, Building 2296, Dhahran, Saudi Aramco 31311, Kingdom of Saudi Arabia.

Author Contributions

All of the experiments were designed and performed by B.G. The manuscript was written by B.G. F.S. suggested some of the original concepts. T.A.H. guided and supervised all activities. All authors have given approval to the final version of the manuscript.

Funding

This work is based upon the work supported by ARPA-E (Advanced Research Projects Agency−Energy) under award no. DE-AR0000083 and by Saudi Aramco under the MIT Energy Initiative program.

Notes

The authors declare no competing financial interest.

ACKNOWLEDGMENTS

We thank Dr. Demetra Achiellos for many helpful discussions on electrochemical processes.

REFERENCES

(1) Wang, W.; Xu, W.; Cosimbescu, L.; Choi, D. W.; Li, L. Y.; Yang, Z. G. Anthraquinone with tailored structure for a nonaqueous metal-organic redox flow battery. *Chem. Commun.* **2012**, *48*, 6669−6671.

(2) Cui, T. B.; Luo, T. L.; Zhang, C.; Li, H. P.; Liu, G. J. Solubilities of 1,4-naphthoquinone in acetone, toluene, xylene, ethanol, and n-butyl alcohol. *J. Chem. Eng. Data* **2008**, *53*, 2254−2257.

(3) Brennecke, J. E.; Gurkan, B. E. Ionic Liquids for CO_2 Capture and Emission Reduction. *J. Phys. Chem. Lett.* **2010**, *1*, 3459−3464.

(4) Rees, N. V.; Compton, R. G. Electrochemical CO_2 sequestration in ionic liquids; a perspective. *Energy Environ. Sci.* **2011**, *4*, 403−408.

(5) Damiani, D.; Litynski, J. T.; McIlvried, H. G.; Vikara, D. M.; Srivastava, R. D. The US Department of Energy's R&D program to reduce greenhouse gas emissions through beneficial uses of carbon dioxide. *Greenhouse Gases: Sci. Technol.* **2012**, *2*, 9−19.

(6) Yang, H. Z.; Gu, Y. L.; Deng, Y. Q.; Shi, F. Electrochemical activation of carbon dioxide in ionic liquid: synthesis of cyclic carbonates at mild reaction conditions. *Chem. Commun.* **2002**, 274−275.

(7) Bard, A. J.; Faulkner, L. R. *Elecrtrochemical Methods: Fundamentals and Applications*, 2nd ed.; Wiley: New York, 2001.

(8) Peng, J. J.; Deng, Y. Q. Cycloaddition of carbon dioxide to propylene oxide catalyzed by ionic liquids. *New J. Chem.* **2001**, *25*, 639−641.

(9) Bachot, J.; Le Roux, O. *Having stable cosolvent insoluble in water but soluble for quinone* **1990**.

(10) Snuffin, L. L.; Whaley, L. W.; Yu, L. Catalytic Electrochemical Reduction of CO_2 in Ionic Liquid $EMIMBF_3Cl$. *J. Electrochem. Soc.* **2011**, *158*, F155−F158.

DOI: 10.1021/acssuschemeng.5b00116
ACS Sustainable Chem. Eng. 2015, 3, 1394−1405

(11) Armand, M.; Endres, F.; MacFarlane, D. R.; Ohno, H.; Scrosati, B. Ionic-liquid materials for the electrochemical challenges of the future. *Nat. Mater.* **2009**, *8*, 621−629.
(12) Galinski, M.; Lewandowski, A.; Stepniak, I. Ionic liquids as electrolytes. *Electrochim. Acta* **2006**, *51*, 5567−5580.
(13) Silvester, D. S.; Compton, R. G. Electrochemistry in room temperature ionic liquids: A review and some possible applications. *Z. Phys. Chem. (Muenchen, Ger.)* **2006**, *220*, 1247−1274.
(14) DuBois, D. L.; Miedaner, A.; Bell, W. L.; Smart, J. C. Electrochemical Concentration of Carbon Dioxide. In *Electrochemical and Electrocatalytic Reactions of Carbon Dioxide*, Sullivan, B. P., Krist, K., Guard, H. E., Eds.; Elsevier: Amsterdam, The Netherlands, 1992; pp 94−117.
(15) Miedaner, A.; Bell, W. L.; Smart, J. C.; Dubois, D. L. Electrochemical Concentration of CO_2 Using Redox Active CO_2 Carrier Molecules. *Abstr. Pap.—Am. Chem. Soc.* **1989**, *198*, 36−Inor.
(16) Tanaka, H.; Nagao, H.; Tanaka, K. Evaluation of Acidity of CO_2 in Protic Media - Carboxylation of Reduced Quinone. *Chem. Lett.* **1993**, 541−544.
(17) Peover, M. E. Reduction Potentials and Intermolecular Charge-Transfer Spectra of Organic Acceptor Molecules 0.1. Quinones. *Trans. Faraday Soc.* **1962**, *58*, 1656−&.
(18) Jaworski, J. S.; Lesniewska, E.; Kalinowski, M. K. Solvent Effect on the Redox Potential of Quinone-Semiquinone Systems. *J. Electroanal. Chem.* **1979**, *105*, 329−334.
(19) Bauscher, M.; Mantele, W. Electrochemical and Infrared-Spectroscopic Characterization of Redox Reactions of P-Quinones. *J. Phys. Chem.* **1992**, *96*, 11101−11108.
(20) Lehmann, M. W.; Evans, D. H. Anomalous behavior in the two-step reduction of quinones in acetonitrile. *J. Electroanal. Chem.* **2001**, *500*, 12−20.
(21) Guin, P. S.; Das, S.; Mandal, P. C. Electrochemical Reduction of Quinones in Different Media: A Review. *Int. J. Electrochem.* **2011**, *2011*, 22.
(22) Tessensohn, M. E.; Hirao, H.; Webster, R. D. Electrochemical Properties of Phenols and Quinones in Organic Solvents are Strongly Influenced by Hydrogen-Bonding with Water. *J. Phys. Chem. C* **2013**, *117*, 1081−1090.
(23) Forsyth, S. A.; Batten, S. R.; Dai, Q.; MacFarlane, D. R. Ionic liquids based on imidazolium and pyrrolidinium salts of the tricyanomethanide anion. *Aust. J. Chem.* **2004**, *57*, 121−124.
(24) Simpson, T. C.; Durand, R. R. Reactivity of Carbon-Dioxide with Quinones. *Electrochim. Acta* **1990**, *35*, 1399−1403.
(25) Gupta, N.; Linschitz, H. Hydrogen-bonding and protonation effects in electrochemistry of quinones in aprotic solvents. *J. Am. Chem. Soc.* **1997**, *119*, 6384−6391.
(26) Russel, C.; Jaenicke, W. Heterogeneous Electron Exchange of Quinones in Aprotic-Solvents 0.4. Influence of Molecular-Structure and Size on the Exchange-Rate Constants of Both Reduction Steps. *J. Electroanal. Chem.* **1986**, *200*, 249−260.
(27) Russel, C.; Jaenicke, W. Heterogeneous Electron-Transfer to Quinones in Aprotic-Solvents 0.2. The Dependence on Solvent and Supporting Electrolyte. *J. Electroanal. Chem.* **1984**, *180*, 205−217.
(28) MacFarlane, D. R.; Forsyth, M.; Izgorodina, E. I.; Abbott, A. P.; Annat, G.; Fraser, K. On the concept of ionicity in ionic liquids. *Phys. Chem. Chem. Phys.* **2009**, *11*, 4962−4967.
(29) Ueno, K.; Tokuda, H.; Watanabe, M. Ionicity in ionic liquids: correlation with ionic structure and physicochemical properties. *Phys. Chem. Chem. Phys.* **2010**, *12*, 1649−1658.
(30) Nikitina, V. A.; Nazmutdinov, R. R.; Tsirlina, G. A. Quinones Electrochemistry in Room-Temperature Ionic Liquids. *J. Phys. Chem. B* **2011**, *115*, 668−677.
(31) Carter, M. T.; Osteryoung, R. A. Interaction of 9,10-Anthraquinone with Tetrachloroaluminate and Proton in Basic Aluminum-Chloride: 1-Ethyl-3-Methylimidazolium Chloride Room-Temperature Molten-Salts. *J. Electrochem. Soc.* **1992**, *139*, 1795−1802.
(32) Wang, Y. J.; Rogers, E. I.; Belding, S. R.; Compton, R. G. The electrochemical reduction of 1,4-benzoquinone in 1-ethyl-3-methyl-imidazolium bis(trifluoromethane-sulfonyl)-imide, [C(2)mim]-[NTf2]: A voltammetric study of the comproportionation between benzoquinone and the benzoquinone dianion. *J. Electroanal. Chem.* **2010**, *648*, 134−142.
(33) Ernst, S.; Aldous, L.; Compton, R. G. The voltammetry of surface bound 2-anthraquinonyl groups in room temperature ionic liquids: Cation size effects. *Chem. Phys. Lett.* **2011**, *511*, 461−465.
(34) Scovazzo, P.; Poshusta, J.; DuBois, D.; Koval, C.; Noble, R. Electrochemical separation and concentration of < 1% carbon dioxide from nitrogen. *J. Electrochem. Soc.* **2003**, *150*, D91−D98.
(35) Barrosse-Antle, L. E.; Bond, A. M.; Compton, R. G.; O'Mahony, A. M.; Rogers, E. I.; Silvester, D. S. Voltammetry in Room Temperature Ionic Liquids: Comparisons and Contrasts with Conventional Electrochemical Solvents. *Chem.—Asian J.* **2010**, *5*, 202−230.
(36) Johnson, B. P.; Gabrielsen, B.; Matulenko, M.; Dorsey, J. G.; Reichardt, C. Solvatochromic Solvent Polarity Measurements in Analytical-Chemistry: Synthesis and Applications of E_T-30. *Anal. Lett.* **1986**, *19*, 939−962.
(37) Mellein, B. R.; Aki, S. N. V. K.; Ladewski, R. L.; Brennecke, J. F. Solvatochromic studies of ionic liquid/organic mixtures. *J. Phys. Chem. B* **2007**, *111*, 131−138.
(38) Zhang, S. J.; Sun, N.; He, X. Z.; Lu, X. M.; Zhang, X. P. Physical properties of ionic liquids: Database and evaluation. *J. Phys. Chem. Ref. Data* **2006**, *35*, 1475−1517.
(39) Noack, K.; Schulz, P. S.; Paape, N.; Kiefer, J.; Wasserscheid, P.; Leipertz, A. The role of the C2 position in interionic interactions of imidazolium based ionic liquids: a vibrational and NMR spectroscopic study. *Phys. Chem. Chem. Phys.* **2010**, *12*, 14153−14161.
(40) Yoshida, Y.; Muroi, K.; Otsuka, A.; Saito, G.; Takahashi, M.; Yoko, T. 1-ethyl-3-methylimidazolium based ionic liquids containing cyano groups: Synthesis, characterization, and crystal structure. *Inorg. Chem.* **2004**, *43*, 1458−1462.
(41) Okoturo, O. O.; VanderNoot, T. J. Temperature dependence of viscosity for room temperature ionic liquids. *J. Electroanal. Chem.* **2004**, *568*, 167−181.
(42) O'Mahony, A. M.; Silvester, D. S.; Aldous, L.; Hardacre, C.; Compton, R. G. Effect of Water on the Electrochemical Window and Potential Limits of Room-Temperature Ionic Liquids. *J. Chem. Eng. Data* **2008**, *53*, 2884−2891.
(43) Yim, T.; Lee, H. Y.; Kim, H. J.; Mun, J.; Kim, S.; Oh, S. M.; Kim, Y. G. Synthesis and properties of pyrrolidinium and piperidinium bis(trifluoromethanesulfonyl)imide ionic liquids with allyl substituents. *Bull. Korean Chem. Soc.* **2007**, *28*, 1567−1572.
(44) Jacquemin, J.; Husson, P.; Padua, A. A. H.; Majer, V. Density and viscosity of several pure and water-saturated ionic liquids. *Green Chem.* **2006**, *8*, 172−180.
(45) Han, H. B.; Nie, J.; Liu, K.; Li, W. K.; Feng, W. F.; Armand, M.; Matsumoto, H.; Zhou, Z. B. Ionic liquids and plastic crystals based on tertiary sulfonium and bis(fluorosulfonyl)imide. *Electrochim. Acta* **2010**, *55*, 1221−1226.
(46) Anthony, J. L.; Maginn, E. J.; Brennecke, J. F. Solution thermodynamics of imidazolium-based ionic liquids and water. *J. Phys. Chem. B* **2001**, *105*, 10942−10949.
(47) Seddon, K. R.; Stark, A.; Torres, M. J. Influence of chloride, water, and organic solvents on the physical properties of ionic liquids. *Pure Appl. Chem.* **2000**, *72*, 2275−2287.
(48) MacFarlane, D. R.; Golding, J.; Forsyth, S.; Forsyth, M.; Deacon, G. B. Low viscosity ionic liquids based on organic salts of the dicyanamide anion. *Chem. Commun.* **2001**, 1430−1431.
(49) Yang, L.; Zhang, Z. X.; Gao, X. H.; Zhang, H. Q.; Mashita, K. Asymmetric sulfonium-based molten salts with TFSI- or PF6- anion as novel electrolytes. *J. Power Sources* **2006**, *162*, 614−619.
(50) Crowhurst, L.; Mawdsley, P. R.; Perez-Arlandis, J. M.; Salter, P. A.; Welton, T. Solvent-solute interactions in ionic liquids. *Phys. Chem. Chem. Phys.* **2003**, *5*, 2790−2794.
(51) Muldoon, M. J.; Gordon, C. M.; Dunkin, I. R. Investigations of solvent-solute interactions in room temperature ionic liquids using solvatochromic dyes. *J. Chem. Soc., Perkin Trans. 2* **2001**, 433−435.

DOI: 10.1021/acssuschemeng.5b00116
ACS Sustainable Chem. Eng. 2015, 3, 1394−1405

(52) Reichardt, C. Pyridinium N-phenoxide betaine dyes and their application to the determination of solvent polarities part 29 - Polarity of ionic liquids determined empirically by means of solvatochromic pyridinium N-phenolate betaine dyes. *Green Chem.* **2005**, *7*, 339−351.
(53) Zhang, S. G.; Qi, X. J.; Ma, X. Y.; Lu, L. J.; Deng, Y. Q. Hydroxyl Ionic Liquids: The Differentiating Effect of Hydroxyl on Polarity due to Ionic Hydrogen Bonds between Hydroxyl and Anions. *J. Phys. Chem. B* **2010**, *114*, 3912−3920.
(54) Tokuda, H.; Tsuzuki, S.; Susan, M. A. B. H.; Hayamizu, K.; Watanabe, M. How ionic are room-temperature ionic liquids? An indicator of the physicochemical properties. *J. Phys. Chem. B* **2006**, *110*, 19593−19600.
(55) Byrne, R.; Fraser, K. J.; Izgorodina, E.; MacFarlane, D. R.; Forsyth, M.; Diamond, D. Photo- and solvatochromic properties of nitrobenzospiropyran in ionic liquids containing the [NTf(2)](−) anion. *Phys. Chem. Chem. Phys.* **2008**, *10*, 5919−5924.
(56) Hayyan, M.; Mjalli, F. S.; Hashim, M. A.; AlNashef, I. M. Generation of Superoxide Ion in Pyridinium, Morpholinium, Ammonium, and Sulfonium-Based Ionic Liquids and the Application in the Destruction of Toxic Chlorinated Phenols. *Ind. Eng. Chem. Res.* **2012**, *51*, 10546−10556.
(57) Walsh, D. A.; Ejigu, A.; Smith, J.; Licence, P. Kinetics and mechanism of oxygen reduction in a protic ionic liquid. *Phys. Chem. Chem. Phys.* **2013**, *15*, 7548−7554.
(58) Anthony, J. L.; Anderson, J. L.; Maginn, E. J.; Brennecke, J. F. Anion effects on gas solubility in ionic liquids. *J. Phys. Chem. B* **2005**, *109*, 6366−6374.
(59) Franco, C.; Olmsted, J. Photochemical Determination of the Solubility of Oxygen in Various Media. *Talanta* **1990**, *37*, 905−909.
(60) Shoup, D.; Szabo, A. Chronoamperometric Current at Finite Disk Electrodes. *J. Electroanal. Chem.* **1982**, *140*, 237−245.
(61) Wang, Y. J.; Belding, S. R.; Rogers, E. I.; Compton, R. G. A kinetic and mechanistic study of the electrochemical oxidation of hydroquinone in 1-ethyl-3-methylimidazolium bis-(trifluoromethanesulfonyl)imide, [C(2)mim][NTf2]. *J. Electroanal. Chem.* **2011**, *650*, 196−204.
(62) Fietkau, N.; Clegg, A. D.; Evans, R. G.; Villagran, C.; Hardacre, C.; Compton, R. G. Electrochemical rate constants in room temperature ionic liquids: The oxidation of a series of ferrocene derivatives. *ChemPhysChem* **2006**, *7*, 1041−1045.
(63) Barrosse-Antle, L. E.; Aldous, L.; Hardacre, C.; Bond, A. M.; Compton, R. G. Dissolved Argon Changes the Rate of Diffusion in Room Temperature Ionic Liquids: Effect of the Presence and Absence of Argon and Nitrogen on the Voltammetry of Ferrocene. *J. Phys. Chem. C* **2009**, *113*, 7750−7754.
(64) Goto, K.; Kodama, S.; Higashii, T. Evaluation of Amine-Based Solvent for Post-Combustion Capture of Carbon Dioxide. *J. Chem. Eng. Jpn.* **2014**, *47*, 663−665.
(65) Song, H.-J.; Lee, S.; Park, K.; Lee, J.; Chand Spah, D.; Park, J.-W.; Filburn, T. P. Simplified Estimation of Regeneration Energy of 30 wt % Sodium Glycinate Solution for Carbon Dioxide Absorption. *Ind. Eng. Chem. Res.* **2008**, *47*, 9925−9930.

DOI: 10.1021/acssuschemeng.5b00116
ACS Sustainable Chem. Eng. 2015, 3, 1394−1405